Biomolecular NMR Assignments
https://doi.org/10.1007/s12104-018-9839-y

ARTICLE

Resonance assignments for the *apo*-form of the cellulose-active lytic polysaccharide monooxygenase *Ta*LPMO9A

Yoshihito Kitaoku[3] · Gaston Courtade[1] · Dejan M. Petrović[2] · Tamo Fukamizo[3] · Vincent G. H. Eijsink[2] · Finn L. Aachmann[1]

Received: 14 May 2018 / Accepted: 9 August 2018

Abstract
The *apo*-form of the 24.4 kDa AA9 family lytic polysaccharide monooxygenase *Ta*LPMO9A from *Thermoascus aurantiacus* has been isotopically labeled and recombinantly expressed in *Pichia pastoris*. In this paper, we report the ^{1}H, ^{13}C, and ^{15}N chemical shift assignments, as well as an analysis of the secondary structure of the protein based on the secondary chemical shifts.

Keywords Lytic polysaccharide monooxygenase · LPMO · AA9 · Cellulose

Biological context

Lytic polysaccharide monooxygenases (LPMOs) are copper-dependent enzymes that cleave polysaccharides (Vaaje-Kolstad et al. 2010, 2017; Quinlan et al. 2011; Meier et al. 2018). LPMOs are classified in the Auxiliary Activity families AA9, AA10, AA11, AA13, AA14 and AA15 (Levasseur et al. 2013; Hemsworth et al. 2014; Vu et al. 2014b; Couturier et al. 2018; Sabbadin et al. 2018) in the Carbohydrate-Active enzyme (CAZy; http://www.cazy.org) database. The discovery of LPMOs in 2010 (Vaaje-Kolstad et al. 2010) has led to extensive research related to their structure, function and diversity (Vaaje-Kolstad et al. 2017; Meier et al. 2018). Because LPMO action increases the susceptibility of recalcitrant substrates such as cellulose and chitin to the action of classical glycoside hydrolases (GHs), LPMOs have become an important ingredient in commercial enzyme cocktails for industrial biomass conversion (Hu et al. 2014; Müller et al. 2015). To create additional insight into LPMO structure and dynamics, and to study substrate binding, several NMR investigations have been conducted (Aachmann et al. 2011, 2012; Courtade et al. 2015, 2016a, b, 2017).

To date, most of the approximately 50 LPMOs that have been characterized are fungal LPMOs belonging to the AA9 family. Fungal LPMOs act on various polysaccharides, including cellulose (Forsberg et al. 2011; Quinlan et al. 2011) xyloglucan and other (1,4)-linked β-glucans (Agger et al. 2014; Bennati-Granier et al. 2015), starch (Vu et al. 2014b; Lo Leggio et al. 2015) and xylan (Frommhagen et al. 2015; Couturier et al. 2018). The regioselectivity of cellulose-active LPMOs varies: they hydroxylate the C1 and/or the C4 in the susceptible glycosidic bond (Quinlan et al. 2011; Isaksen et al. 2014; Vu et al. 2014a). Structural characterization of the active site of LPMOs has shown that the copper ion in the active site is coordinated by a highly conserved "histidine brace" formed by three nitrogen ligands provided by the N-terminal amino group and the side-chains of the N-terminal histidine ($N^{\delta1}$; His1) and a more distal histidine ($N^{\varepsilon2}$) (Quinlan et al. 2011).

In early work on LPMOs, an AA9 from *Thermoascus aurantiacus* (*Ta*LPMO9A, previously known as *Ta*GH61A) received much attention, and functional data indicate that its inclusion in cellulolytic enzyme cocktails is highly beneficial for overall processing efficiency (Müller et al. 2015; Chylenski et al. 2017). Thus, this enzyme is an interesting

Yoshihito Kitaoku and Gaston Courtade have contributed equally to this work.

✉ Finn L. Aachmann
finn.l.aachmann@ntnu.no

[1] NOBIPOL, Department of Biotechnology and Food Science, NTNU Norwegian University of Science and Technology, Sem Sælands vei 6/8, 7491 Trondheim, Norway

[2] Faculty of Chemistry, Biotechnology and Food Science, Norwegian University of Life Sciences, 1432 Ås, Norway

[3] Biochemistry-Electrochemistry Research Unit, Institute of Science, Suranaree University of Technology, Nakhon Ratchasima 30000, Thailand

Published online: 16 August 2018

candidate for future investigations. The X-ray diffraction structure (PDB ID: 3ZUD) of *Ta*LPMO9A has been published (Quinlan et al. 2011). The structure displays the typical fibronectin type III LPMO fold composed of two β-sheets (one 3-stranded and one 4-stranded) from which several loops protrude. The NMR assignment data presented here will allow future structural and functional studies on the *apo*-form of *Ta*LPMO9A, including studies on enzyme-substrate interactions that are not feasible through X-ray crystallography (Aachmann et al. 2012; Courtade et al. 2016b).

Methods and experiments

The NMR assignment was performed on the *apo*-form of the recombinantly expressed *Ta*LPMO9A. *Ta*LPMO9A was cloned in *Pichia pastoris* as described before (Chylenski et al. 2017), and production of the isotopically labeled *Ta*LPMO9A was done following previously published protocol (Pickford and O'Leary 2004). In summary, *P. pastoris* harboring the *Ta*-LPMO9A gene inserted into the pPinkGAP vector (Várnai et al. 2014) was grown in 50 mL of ^{13}C, ^{15}N-labeled buffered minimal glucose medium (^{13}C, ^{15}N-BMD), composed of 0.34% (w/v) yeast nitrogen base without amino acids or ammonium sulfate (Becton, Dickinson & Company, MD, USA), 0.5% (w/v) ^{13}C-labeled glucose (Synthose Inc, Ontario, Canada), 1% (w/v) ^{15}N-labeled ammonium sulfate (Sigma-Aldrich, MO, USA), 4×10^{-5} % (w/v) biotin (Sigma-Aldrich, MO, USA) in 100 mM potassium phosphate buffer pH 6.0, in a 250-mL shake flask at 29 °C and 200 rpm for 24 h. Subsequently, the culture was used to inoculate 450 mL ^{13}C, ^{15}N-BMD medium in 2 L shake flasks followed by incubation at 29 °C and 200 rpm for 48 h. After the first 24 h, the medium was re-supplemented with 1% (w/v) ^{13}C-labeled glucose. The culture was centrifuged at 7000×*g* for 15 min at 4 °C to remove the cells. The supernatant was dialyzed against 50 mM Bis-Tris buffer, pH 6.5, and concentrated to 100 mL using a VivaFlow 50 tangential crossflow concentrator (MWCO 10 kDa, Sartorius Stedim Biotech GmbH, Goettingen, Germany). Ammonium sulfate was added to the concentrated supernatant to a final concentration of 1.42 M prior to loading onto a 5-mL HiTrap Phenyl FF column (GE Healthcare, Uppsala, Sweden), equilibrated with 50 mM Bis-Tris buffer (pH 6.5) containing 1.42 M ammonium sulfate, using a flow rate of 1 mL min^{-1}. Proteins were eluted using a 25 mL linear gradient from 1.42 to 0 M ammonium sulfate in 50 mM Bis-Tris buffer (pH 6.5). Fractions containing the pure protein were identified using SDS-PAGE and subsequently pooled, concentrated and buffer exchanged to 50 mM Bis-Tris buffer, pH 6.5, using Amicon Ultra centrifugal filters (MWCO 3 kDa, Merck Millipore, NJ, USA). The *apo*-form of *Ta*LPMO9A was obtained by incubating the protein sample with 10 mM Na-EDTA for 45 min at room temperature, followed by buffer exchange to 25 mM ammonium acetate buffer, pH 6.5, using Amicon Ultra centrifugal filters (MWCO 3 kDa, Merck Millipore, NJ, USA).

The NMR spectra were recorded at 25 °C on a Bruker Ascend 800 MHz spectrometer Avance III HD equipped with a 5 mm Z-gradient CP-TCI (H/C/N) cryoprobe at the NV-NMR-Center/Norwegian NMR Platform in Trondheim, Norway. ^{1}H shifts were referenced internally to the water signal, while ^{13}C and ^{15}N chemical shifts were referenced indirectly to water, based on the absolute frequency ratios (Zhang et al. 2003). Sequence-specific backbone and side-chain assignments of *Ta*LPMO9A were accomplished using ^{15}N-HSQC, ^{13}C-aliphatic HSQC, ^{13}C-aromatic HSQC, HNCO, HN(CA)CO, HNCA, CBCA(CO)NH, HBHA(CO)NH, HC(C)H-TOCSY, ^{15}N-edited NOESY–HSQC, and ^{13}C-edited aliphatic and aromatic NOESY–HSQC spectra. The NMR data was recorded and processed with Bruker TopSpin version 3.5 and spectral analysis was performed using CARA version 1.5.5 (Keller 2004). Secondary structure elements were analyzed using the web-based version of the TALOS-N software (http://spin.niddk.nih.gov/bax/software/TALOS-N/) (Shen and Bax 2013) using the ^{13}C and ^{15}N chemical shifts. Secondary structure propensity was also analyzed using secondary structure propensities (SSP from chemical shifts) (Marsh et al. 2006).

Assignment and data deposition

We report here the assignment of the backbone and side-chain resonances of *Ta*LPMO9A (HN, N, Cα, C′ > 95%; aliphatic side-chains > 79%). The ^{15}N-HSQC spectrum, together with the assignment of the resonances is shown in Fig. 1. Because of fast exchange, the N-terminal amino group of His1 could not be found, whereas other nuclei of this residue ($C^{\varepsilon1}$/$H^{\varepsilon1}$) were assigned. His1 in *apo*-LPMOs has been shown to have higher conformational flexibility than in metal-loaded LPMOs (Aachmann et al. 2012), and, as a consequence of this, its side-chain signals are observed as narrow, intense peaks. Additional evidence supporting the assignment of His1 was thus obtained by analysis of the aromatic region of the ^{13}C-HSQC spectrum. Indeed, the most intense peak matched the assignment (obtained primarily using the ^{13}C-edited NOESY spectrum) of the side-chain ($C^{\varepsilon1}$/$H^{\varepsilon1}$) of His1. Furthermore, addition of 0.6 mM Cu(II) SO_4 caused the signals assigned to His1 and His86 to vanish, due to the paramagnetic relaxation enhancement brought about by the presence of paramagnetic Cu^{2+} less than 10 Å away from the coordinating histidines (Bertini and Pierattelli 2004). Exchangeable side-chain protons were not assigned, nor were the amide side-chain protons of Asn and Gln. For the aromatic side-chains, assignment of the side-chain $C^{\varepsilon1}$/

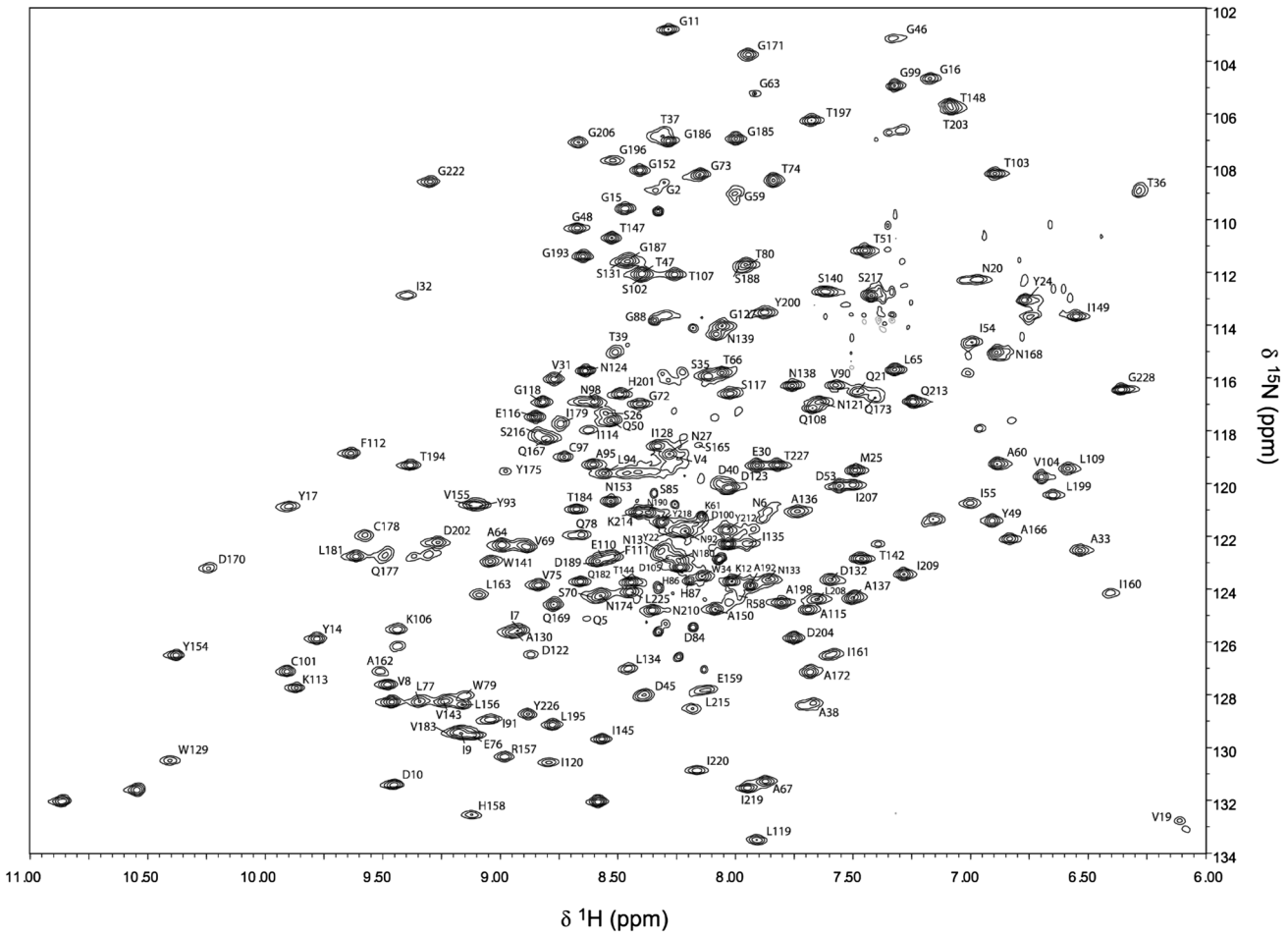

Fig. 11 H, ^{15}N HSQC spectrum of ^{13}C, ^{15}N-labeled *apo-Ta*LPMO9A (0.2 mM) from *T. auranticus* in (90:10) H_2O:D_2O in 25 mM ammonium acetate buffer, pH 6.5, at 298 K. Residue types and numbers are indicated

$H^{\varepsilon 1}$ histidine pairs was prioritized and successful, whereas other aromatic side-chains were not assigned. The chemical shift data has been deposited in the Biological Magnetic Resonance Data Bank (BMRB) under the accession code 27,411.

Analysis of the secondary structure elements of *Ta*LPMO9A indicated the presence of 8–9 β-strands (Fig. 2) and three helical stretches. The length and position of most the secondary structure elements are in good agreement with those observed in the X-ray crystal diffraction structure of

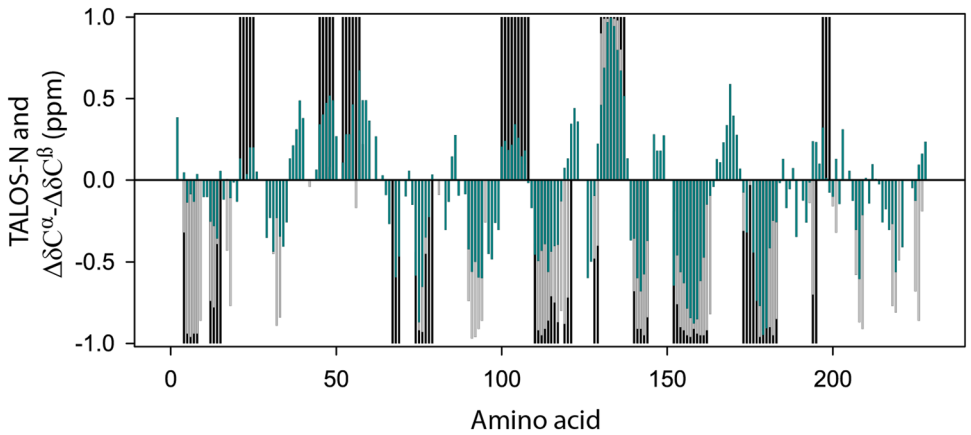

Fig. 2 Secondary structure propensity of *Ta*LPMO9A analyzed by TALOS-N (grey) and $\Delta\delta C^{\alpha} - \Delta\delta C^{\beta}$ secondary chemical shifts (SSP approach; teal) together with the secondary structure elements from the X-ray crystal diffraction structure of *Ta*LPMO9A (PDB ID: 3ZUD; black). Positive values indicate helical propensity and negative values indicate β-strand propensity

*Ta*LPMO9A (PDB ID: 3ZUD) (Quinlan et al. 2011). A few helical structures (res 21–25, 45–57 and 100–108), which are present in the crystal structure, were not identified by TALOS-N, whereas the SSP approach showed a slight helical propensity for those regions. The extended stretch of residues 215–228, was identified as such by both TALOS-N and SSP (Fig. 2) in good agreement with the X-ray crystal diffraction structure of *Ta*LPMO9A. Interestingly, this stretch is not assigned as a β-strands element even though it would appear to be antiparallel to the β-strand comprising residues 110–121.

Acknowledgements This work was financed by SO-funds from NTNU Norwegian University of Science and Technology and by the "Advancing biomass technology—a biomimetic approach" project, the KIFEE project and the Norwegian NMR Platform, all from the Research Council of Norway (Grant Nos. 243663, 249797, 226244, respectively).

Compliance with ethical standards

Conflict of interest The authors declare that they have no conflict of interest.

References

Aachmann FL, Eijsink VGH, Vaaje-Kolstad G (2011) ^{1}H, ^{13}C, ^{15}N resonance assignment of the chitin-binding protein CBP21 from *Serratia marcescens*. Biomol NMR Assign 5:117–119. https://doi.org/10.1007/s12104-010-9281-2

Aachmann FL, Sørlie M, Skjåk-Bræk G et al (2012) NMR structure of a lytic polysaccharide monooxygenase provides insight into copper binding, protein dynamics, and substrate interactions. Proc Natl Acad Sci USA 109:18779–18784. https://doi.org/10.1073/pnas.1208822109

Agger JW, Isaksen T, Várnai A et al (2014) Discovery of LPMO activity on hemicelluloses shows the importance of oxidative processes in plant cell wall degradation. Proc Natl Acad Sci USA 111:6287–6292. https://doi.org/10.1073/pnas.1323629111

Bennati-Granier C, Garajova S, Champion C et al (2015) Substrate specificity and regioselectivity of fungal AA9 lytic polysaccharide monooxygenases secreted by *Podospora anserina*. Biotechnol Biofuels 8:90. https://doi.org/10.1186/s13068-015-0274-3

Bertini I, Pierattelli R (2004) Copper(II) proteins are amenable for NMR investigations. Pure Appl Chem 76:321–333. https://doi.org/10.1351/pac200476020321

Chylenski P, Petrović DM, Müller G et al (2017) Enzymatic degradation of sulfite-pulped softwoods and the role of LPMOs. Biotechnol Biofuels 10:1–13. https://doi.org/10.1186/s13068-017-0862-5

Courtade G, Balzer S, Forsberg Z et al (2015) ^{1}H, ^{13}C, ^{15}N resonance assignment of the chitin-active lytic polysaccharide monooxygenase *Bl*LPMO10A from *Bacillus licheniformis*. Biomol NMR Assign 9:207–210. https://doi.org/10.1007/s12104-014-9575-x

Courtade G, Wimmer R, Dimarogona M et al (2016a) Backbone and side-chain ^{1}H, ^{13}C, and ^{15}N chemical shift assignments for the *apo*-form of the lytic polysaccharide monooxygenase *Nc*LPMO9C. Biomol NMR Assign 10:277–280. https://doi.org/10.1007/s12104-016-9683-x

Courtade G, Wimmer R, Røhr ÅK et al (2016b) Interactions of a fungal lytic polysaccharide monooxygenase with β-glucan substrates and cellobiose dehydrogenase. Proc Natl Acad Sci USA 113:5922–5927. https://doi.org/10.1073/pnas.1602566113

Courtade G, Forsberg Z, Vaaje-Kolstad G et al (2017) Chemical shift assignments for the *apo*-form of the catalytic domain, the linker region, and the carbohydrate-binding domain of the cellulose-active lytic polysaccharide monooxygenase *Sc*LPMO10C. Biomol NMR Assign 11:257–264. https://doi.org/10.1007/s12104-017-9759-2

Couturier M, Ladevèze S, Sulzenbacher G et al (2018) Lytic xylan oxidases from wood-decay fungi unlock biomass degradation. Nat Chem Biol 14:306–310. https://doi.org/10.1038/nchembio.2558

Forsberg Z, Vaaje-Kolstad G, Westereng B et al (2011) Cleavage of cellulose by a CBM33 protein. Protein Sci 20:1479–1483. https://doi.org/10.1002/pro.689

Frommhagen M, Sforza S, Westphal AH et al (2015) Discovery of the combined oxidative cleavage of plant xylan and cellulose by a new fungal polysaccharide monooxygenase. Biotechnol Biofuels 8:101. https://doi.org/10.1186/s13068-015-0284-1

Hemsworth GR, Henrissat B, Davies GJ, Walton PH (2014) Discovery and characterization of a new family of lytic polysaccharide monooxygenases. Nat Chem Biol 10:122–126. https://doi.org/10.1038/nchembio.1417

Hu J, Arantes V, Pribowo A (2014) Substrate factors that influence the synergistic interaction of AA9 and cellulases during the enzymatic hydrolysis of biomass. Energy Environ Sci 7:2308–2315. https://doi.org/10.1039/C4EE00891J

Isaksen T, Westereng B, Aachmann FL et al (2014) A C4-oxidizing lytic polysaccharide monooxygenase cleaving both cellulose and cello-oligosaccharides. J Biol Chem 289:2632–2642. https://doi.org/10.1074/jbc.M113.530196

Keller R (2004) The computer aided resonance assignment tutorial. CANTINA Verlag, Goldau

Levasseur A, Drula E, Lombard V et al (2013) Expansion of the enzymatic repertoire of the CAZy database to integrate auxiliary redox enzymes. Biotechnol Biofuels 6:41–54. https://doi.org/10.1186/1754-6834-6-41

Lo Leggio L, Simmons TJ, Poulsen JN et al (2015) Structure and boosting activity of a starch-degrading lytic polysaccharide monooxygenase. Nat Commun 6:1–9. https://doi.org/10.1038/ncomms6961

Marsh J, Singh VK, Jia Z, Forman-Kay JD (2006) Sensitivity of secondary structure propensities to sequence differences between alpha- and gamma-synuclein: implications for fibrillation. Protein Sci 15:2795–2804. https://doi.org/10.1110/ps.062465306

Meier KK, Jones SM, Kaper T et al (2018) Oxygen activation by Cu LPMOs in recalcitrant carbohydrate polysaccharide conversion to monomer sugars. Chem Rev 118:2593–2635. https://doi.org/10.1021/acs.chemrev.7b00421

Müller G, Várnai A, Johansen KS et al (2015) Harnessing the potential of LPMO-containing cellulase cocktails poses new demands on processing conditions. Biotechnol Biofuels 8:187. https://doi.org/10.1186/s13068-015-0376-y

Pickford AR, O'Leary JM (2004) Isotopic labeling of recombinant proteins from the methylotrophic yeast *Pichia pastoris*. Methods Mol Biol 278:17–33. https://doi.org/10.1385/1-59259-809-9:017

Quinlan RJ, Sweeney MD, Lo Leggio L et al (2011) Insights into the oxidative degradation of cellulose by a copper metalloenzyme that exploits biomass components. Proc Natl Acad Sci USA 108:15079–15084. https://doi.org/10.1073/pnas.1105776108

Sabbadin F, Hemsworth GR, Ciano L et al (2018) An ancient family of lytic polysaccharide monooxygenases with roles in arthropod development and biomass digestion. Nat Commun 9:756. https://doi.org/10.1038/s41467-018-03142-x

Shen Y, Bax A (2013) Protein backbone and sidechain torsion angles predicted from NMR chemical shifts using artificial neural networks. J Biomol NMR 56:227–241. https://doi.org/10.1007/s10858-013-9741-y

Vaaje-Kolstad G, Westereng B, Horn SJ et al (2010) An oxidative enzyme boosting the enzymatic conversion of recalcitrant polysaccharides. Science 330:219–222. https://doi.org/10.1126/science.1192231

Vaaje-Kolstad G, Forsberg Z, Loose JS et al (2017) Structural diversity of lytic polysaccharide monooxygenases. Curr Opin Struct Biol 44:67–76. https://doi.org/10.1016/j.sbi.2016.12.012

Várnai A, Tang C, Bengtsson O et al (2014) Expression of endoglucanases in *Pichia pastoris* under control of the GAP promoter. Microb Cell Fact 13:1–10. https://doi.org/10.1186/1475-2859-13-57

Vu VV, Beeson WT, Phillips CM et al (2014a) Determinants of regioselective hydroxylation in the fungal polysaccharide monooxygenases. J Am Chem Soc 2:562–565. https://doi.org/10.1021/ja409384b

Vu VV, Beeson WT, Span EA et al (2014b) A family of starch-active polysaccharide monooxygenases. Proc Natl Acad Sci USA 111:13822–13827. https://doi.org/10.1073/pnas.1408090111

Zhang H, Neal S, Wishart DS (2003) RefDB: a database of uniformly referenced protein chemical shifts. J Biomol NMR 25:173–195. https://doi.org/10.1023/A:1022836027055